

MIT Open Access Articles

Transdermal drug delivery by localized intervention

The MIT Faculty has made this article openly available. **Please share** how this access benefits you. Your story matters.

Citation: Gowrishankar, T.R., T.O. Herndon, and J.C. Weaver. "Transdermal drug delivery by localized intervention." *Engineering in Medicine and Biology Magazine*, IEEE 28.1 (2009): 55-63.
© Copyright 2009 IEEE

As Published: <http://dx.doi.org/10.1109/MEMB.2008.931016>

Publisher: Institute of Electrical and Electronics Engineers

Persistent URL: <http://hdl.handle.net/1721.1/52351>

Version: Final published version: final published article, as it appeared in a journal, conference proceedings, or other formally published context

Terms of Use: Article is made available in accordance with the publisher's policy and may be subject to US copyright law. Please refer to the publisher's site for terms of use.





© BRAND X PICTURES

Transdermal Drug Delivery by Localized Intervention

Field-Confined Skin Electroporation and Dermal Microscissioning

BY T.R. GOWRISHANKAR,
TERRY O. HERNDON,
AND JAMES C. WEAVER

Oral and needle-based administration of drugs have long been accepted as a simple, convenient, and inexpensive mode of drug delivery. However, the systemic delivery of drugs degrades the compound during its passage through the low pH environment of the gastrointestinal (GI) tract. Also, these methods are not suited for the delivery of new and highly complex drugs. In addition, other concerns such as protection from needle-prick injuries, need for sustained delivery, and relief for needle-phobic patients have risen sharply. Several alternatives have been developed in the past few decades. These include pulmonary, transmucosal, transdermal, and buccal routes of delivery. These methods provide the advantages of local and minimally invasive delivery and are suited for the delivery of specific drugs.

Transdermal drug delivery systems have the potential to make a major impact on the way both traditional drugs and novel pharmaceuticals are administered. The skin offers an unobtrusive route for drug delivery, which encourages patients' compliance in taking medication. A variety of low-molecular-weight (<300 Da) drugs are delivered by transdermal patches that utilize preexisting pathways in the skin, such as sweat ducts and hair follicles. However, the barrier properties of the stratum corneum (SC), the outermost layer of the skin, limit the rate, size, and type of molecules that can be delivered by patches. A number of active transdermal methods have been developed to enhance the rate of drug delivery by physical or chemical intervention [1], [2].

Chemical permeation enhancers are widely used to enhance the transport of drugs across the skin [3], [4]. Several physical means have been demonstrated to increase the throughput of small and macromolecules across the skin. For example, iontophoresis employs low-level electrical current to deliver drugs through the skin [5]. Low-frequency ultrasonic energy is used in sonophoresis to produce cavitation bubbles that create microchannels in the skin, through which drugs are delivered [6], [7]. Thermal poration creates small open pits by local heating [8]. Laser-ablated SC allows drugs to penetrate the skin [9]. Microneedles are used to penetrate the outer layers of the skin to provide pathways for drug delivery [10], [11]. In many needle-free devices, drugs in powder form enter the skin ballistically at a speed of up to 750 m/s [12].

Patient compliance in transdermal drug delivery that utilizes physical means will greatly improve if the intervention is localized and minimally invasive. We have previously shown that transdermal drug delivery by electroporation can be constrained to occur in local areas on the skin using an insulating mask with well-defined microholes [13]–[15]. Here, we describe two approaches to spatially localized transdermal drug delivery: field-confined skin electroporation and microscissioning. The first method employs field-confining electrodes to apply high-voltage (HV) electrical pulses to create openings in the outer layers of skin [16]. The second method creates small openings (microconduits) through the SC and epidermis by controlled removal of skin by a moderate-velocity particle stream [17].

Field-Confined Skin Electroporation

Skin Electroporation

Skin electroporation [18] extends the concept of lipid bilayer membrane electroporation [19], in which a transient elevation of the transmembrane voltage is hypothesized to create aqueous pathways across the multilamellar bilayer membranes of the SC [20]. These pathways were shown to enhance the delivery of low-molecular-weight molecules (<1 kDa) but showed only a limited increase in macromolecular flux. The keratin matrix within the corneocytes acts as a sieve in trapping large molecules. Electroporation was then used to introduce low-toxicity keratolytic molecules into the corneocytes to disrupt the keratin matrix. The combination of new aqueous pathways through the multilamellar lipid bilayer membranes and disruption of the keratin matrix results in dislodgement of entire stacks of corneocytes, creating microconduits through the SC [14], [15], [20], [21].

We have previously shown that electroporation could be constrained to occur at predetermined sites (microholes in a thin insulating sheet), even with imperfect skin contact [13]. In these studies, an insulating sheet containing an array of microholes (50–150 μm diameter) that contacted the skin forced the electric field to penetrate the skin mainly through the regions exposed to the microholes. Using keratolytic molecules in conjunction with such localized electroporation, we created microconduits with a minimum size of 50 μm diameter. Such openings present a negligible steric hindrance to macromolecule transport. Microconduits were shown to support volumetric flow in the order of 0.01 mL/s by a pressure

Digital Object Identifier 10.1109/EMEB.2008.931016

Patient compliance in transdermal drug delivery that utilizes physical means will greatly improve if the intervention is localized and minimally invasive.

difference of only 0.01 atm (about 10^2 Pa), demonstrating that the SC barrier had been completely removed within this microscopic area [14], [15].

Currently, skin electroporation employs HV pulses applied across skin pleats or between two sites on the skin. This causes the resulting electric field to penetrate deep into the skin, stimulating the underlying nerves. These fields may therefore cause involuntary muscle contraction and pain. To make skin electroporation a viable technology for transdermal drug delivery and analyte sampling, it should cause minimal sensation [16]. Here, we show that field-confined skin electroporation enables drug delivery with reduced sensation.

Transverse and Lateral Electroporation

Skin electroporation is achieved by applying HV electrical pulses across the skin using a pair of electrodes. Depending on the relative orientation of these electrodes, the resulting electroporation can predominantly be either transverse or lateral (Figure 1). In transverse electroporation, the electrodes are far apart (compared with the thickness of the insulating barrier of SC, which is approximately $20\text{ }\mu\text{m}$), causing the field lines between the electrodes to penetrate deep into the skin. Such an arrangement would cause electroporation of SC, epidermis, and possibly deeper tissue. This would lead to muscle contraction and nerve stimulation. When the distance between the electrodes is small ($<200\text{--}300\text{ }\mu\text{m}$), the field lines travel from one electrode to another mainly through the superficial layers of the skin. This causes lateral electroporation of the SC and epidermal cells that lie between the electrodes. Because the main barrier for transdermal drug delivery is the SC, confining the electric field mostly to the SC by optimizing the electrode arrangement is beneficial (Figure 1).

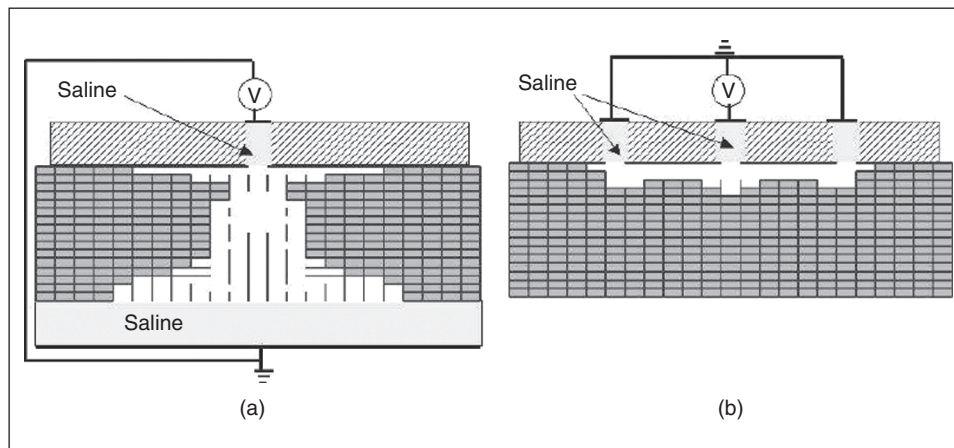


Fig. 1. Illustration of (a) lateral and (b) transverse SC electroporation near one microhole of a two-dimensional (2-D) Cartesian ERD. A brick wall model of the outer layers of the skin was constructed using a 2-D array of resistors. The array of rectangles represents the corneocytes (bricks) of an idealized SC. The dark lines between corneocytes are multilamellar (here six bilayers) lipid barriers. The white regions are corneocytes that have at least one electroporated barrier. For an applied field, the voltages at different nodes were computed using simulation program with integrated circuit emphasis (SPICE) circuit solver. An extension of this method allows a general description of electrical fields and local interactions (30). Those resistors that had a voltage greater than an electroporation threshold (1 V) were designated as representing electroporated segments (shown in white). When a segment was electroporated, fields and current were redistributed, and the model solution evolved in time achieving the pattern shown here. A central slot filled with electrolyte replaces the central cylindrical region of an ERD. Two different electrode arrangements were investigated by applying a 50-V pulse between the electrodes. (a) The outer electrolyte-filled slot contacts the annular active electrode of a cylindrical ERD. The planar counter electrode contacts the dermis. Predominantly, transverse electroporation from the electric field penetrating deep into the skin is seen (16). (b) The overlying hatched gray region with three white slots represents the 2-D equivalent of an ERD annular electrode with an electrically insulating thin sheet. The electrolyte-filled central slot contacts the active electrode, while the outer two slots contacts the annular counter electrode. Predominantly, lateral electroporation results from the confinement of the electric field to the outermost layers of the skin. The extent and location of electroporated segments within the SC will depend on the configuration of the ERD microholes and concentric microelectrodes, together with the HV pulse magnitude, pulse time dependence, and resulting local temperature rise (31).

Field-Confining Electrodes

The concept of lateral electroporation was applied in designing the electrodes of an electrode-reservoir device (ERD) to confine the electric field to SC (Figure 2). An insulating sheet with a conductive coating that contacts the skin serves as one electrode. The second electrode is kept away from the skin, with the intervening region filled with conducting fluid. The insulating sheet contains one or more holes, with an insulating annular region around the periphery. When the skin makes close contact with the sheet, the electric field is forced to go through the skin to reach the counterelectrode. The dimension of the annular region relative to the SC thickness controls the depth of penetration of the electric field.

Electrode Array Fabrication

The electrode arrays were fabricated with a 50- μm thick polyimide (PI) sheet (DuPont V-Film Kapton). One side of the film was microroughened by oxygen plasma etching for 1–2 min. A 150- \AA thick bonding layer of chrome was then electron-beam deposited on the etched side, followed by the deposition of a 3,000- \AA thick layer of gold. An infrared (1,047 nm) laser mounted on a high-speed, 0.1 μm accuracy, x - y positioning system was used to open microholes selectively in the gold/chrome layer. Microholes were generated by repositioning the gold-coated PI in the pulsed laser beam repeatedly, opening overlapping concentric circles in the metal. One pulse per position clearly opened a 15- μm diameter microhole in the metal. A 200- μm diameter microhole required two concentric circles of eight and 16 microholes, respectively. A multiline (centered at 514 nm) green laser on a similar computer-controlled x - y table system was used to make the microholes through the PI. Residues in the PI microholes were removed using either a 1-min ultrasonic cleanup in water or an oxygen

plasma etch. PI films having one microhole to arrays of 121 microholes containing 20–200- μm diameter PI microholes and 40–500- μm diameter gold microholes on 300–800- μm centers were fabricated. The completed film and electrode arrays were cut to fit the electrode holder.

In Vitro Drug Delivery

Two fluorescent model molecules, viz., calcein and sulforhodamine, were used to assess transdermal delivery in vitro by lateral and transverse electroporation. A piece of full-thickness human skin was used with an ERD (Figures 1 and 2), with an 11×11 array of 65- μm diameter microholes. The annular gap between a microhole and the thin film gold electrode was 140 μm , with a 500- μm microhole-to-microhole separation. A series of 360 exponentially decaying pulses ($\tau = 0.6$ ms) of magnitude 260 V was applied. Figure 3(a) shows that the dye was delivered locally within the SC in the region exposed to the microholes in the insulating sheet. The array of bright spots in the skin [shown in more detail in Figure 3(b)]

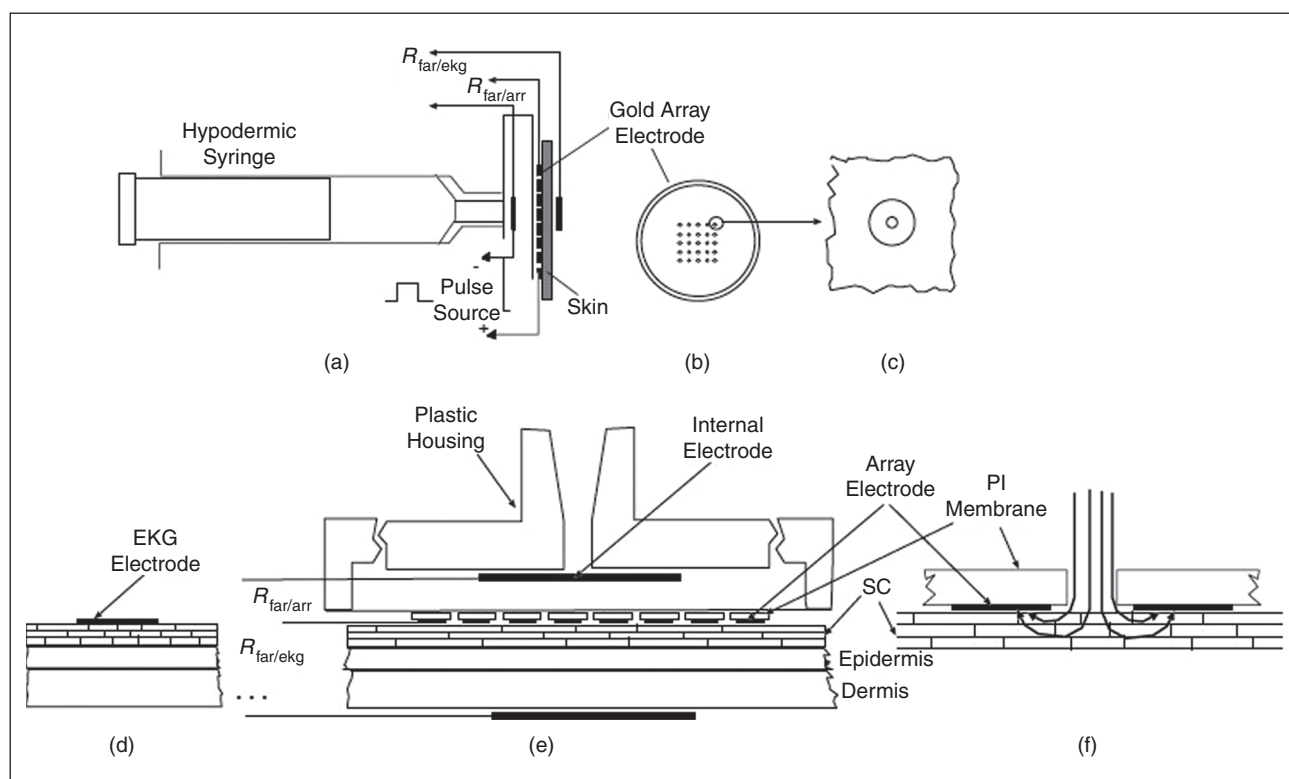


Fig. 2. Main features of a prototype microelectrode-based ERD for painless skin electroporation. (a) ERD attached to syringe, with electrical leads (arrows) leading to a pulse source; $R_{\text{far/arr}}$ = resistance between far (internal) electrode and the gold film array electrode; $R_{\text{far/ECG}}$ = resistance between internal electrode and an electrocardiogram (ECG) electrode (see (d)). (b) Top or bottom view of gold film electrode with an array of microholes. (c) Enlarged view of one hole in gold electrode, with an annular gap and a smaller through-PI microhole (filled with phosphate buffered saline (PBS) or donor solution). (d) ECG electrode (in vivo experiments) located about 20 cm away. Negligible electrical conduction across the intervening dry skin was measured. $R_{\text{far/ECG}}$ involves a pathway from the internal electrode (see (e)) through the skin at the sites of the microholes, through the underlying tissue (only about 100 Ω) and across the skin at the ECG electrode (about 2,000 Ω). A decrease in the total resistance of this pathway indicates the electroporation of the skin in the slot. (e) Main portion of an ERD, showing the housing, internal electrode within the solution reservoir, PI membrane (f), the gold film electrode, and the skin (SC, epidermis, and dermis). The reservoir can contain molecules to be transported across the skin or can serve as a receptor volume for molecules taken out across the skin. (f) Enlarged view of one microhole, annular gap, and SC-contacting gold film electrode. The descending curved lines terminating in arrows show (one polarity) the local electric field (and current) lines, which are confined mainly to the SC. In transverse electroporation experiments, the electrode on the dermis side (e) was used as a counterelectrode. HV pulses were delivered by discharging a capacitor between the pulse source terminals.

Because the main barrier for transdermal drug delivery is the SC, confining the electric field mostly to the SC by optimizing the electrode arrangement is beneficial.

coincided with the array of microholes in the electrode sheet. Two different electrode arrangements were tested. In the first arrangement, the gold sheet served as an electrode, corresponding to the case of lateral electroporation. The resulting fluorescence distribution, as seen in the skin cross section [Figure 3(c)], confirms lateral electroporation. The dye is

localized to the outer layer of the skin directly below the annular gap in the electrode. In the second arrangement, the second electrode is placed on the dermis side of the skin specimen, conducive for transverse electroporation. The fluorescent molecules, in this case, are delivered as deep as 80 μm below the skin surface [Figure 3(d)]. This result is consistent with the

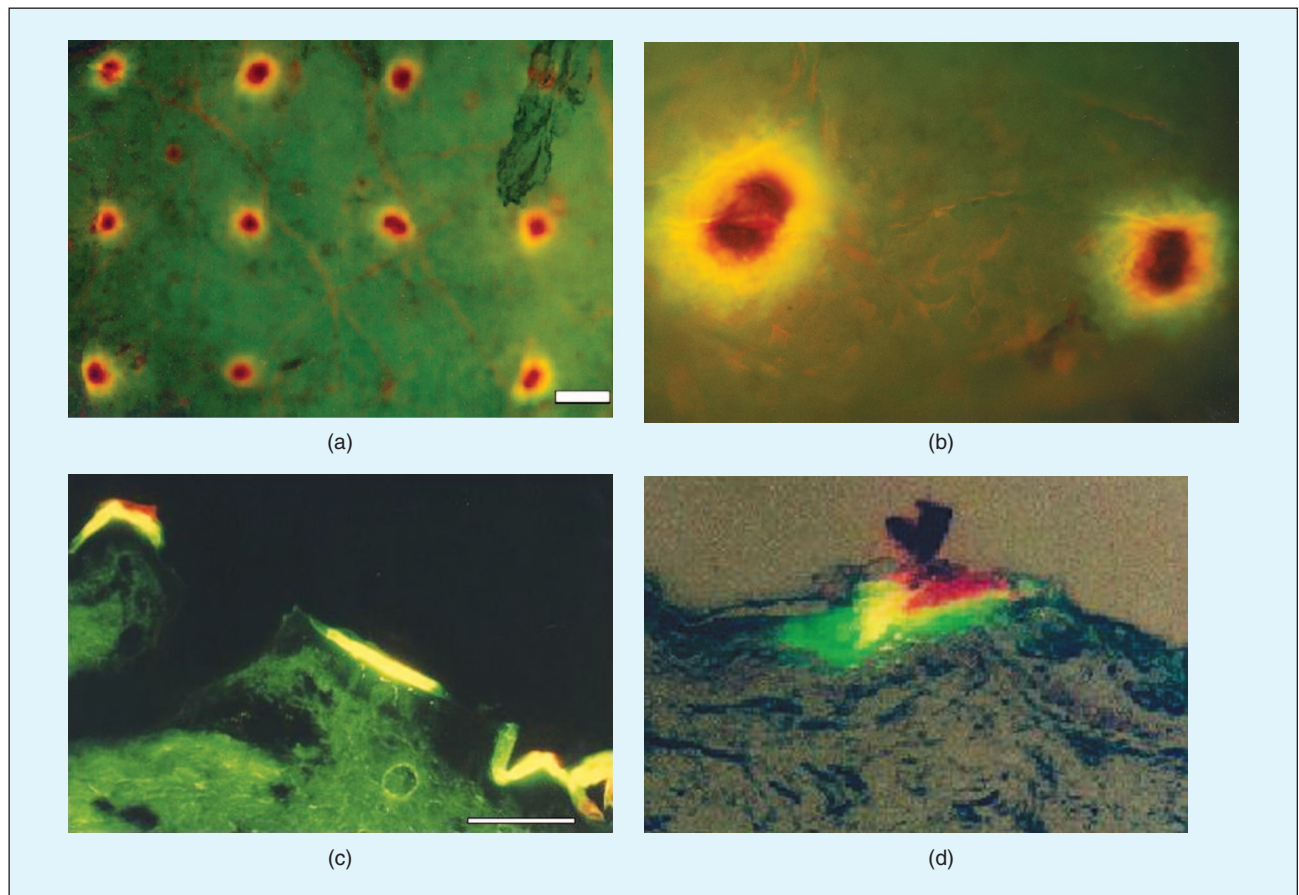


Fig. 3. Delivery of fluorescent molecules into the SC of full-thickness human skin in vitro by an ERD, with an 11×11 array of $65\text{-}\mu\text{m}$ diameter microholes. The annular gap between a microhole and the thin film gold electrode is $140\text{ }\mu\text{m}$, with a $500\text{-}\mu\text{m}$ microhole-to-microhole separation. A total of 360 exponentially decaying pulses ($\tau = 0.6\text{ ms}$; 260 V) was applied. The ERD reservoir medium contained two fluorescent molecules: 1 mM calcein (charge, -4 ; molecular weight, 623) and 1 mM sulforhodamine (charge, -1 ; molecular weight, 607). The skin was secured either from the abdomen, arm, or back of adult human cadavers (National Disease Research Interchange (NDRI), Philadelphia, Pennsylvania; Ohio Valley Tissue and Skin Center, Cincinnati, Ohio)). (a) Top view of skin by fluorescence microscopy. Dark spots (red fluorescence of sulforhodamine) at the $500\text{-}\mu\text{m}$ spacing are surrounded by light rings (green fluorescence of calcein). The autofluorescence of the skin is seen as a diffuse green background. (b) Magnified image of two sites from the array. The dark center and surrounding ring regions are evident. (c) Cross section of microtomed ($10\text{-}\mu\text{m}$ -thick sections) skin specimen (scale bar, $100\text{ }\mu\text{m}$). This shows fluorescence within the SC at distances corresponding to the $500\text{-}\mu\text{m}$ separation ($10\times$ magnification). This localized fluorescence is consistent with predominantly lateral electroporation. (d) A similarly sectioned skin shows penetration of dyes deeper into the skin for the transverse skin electroporation configuration (Figure 2).

electroporation of skin clamped in a side-by-side chamber [13]. Lateral skin electroporation was evident from the large decrease in skin resistance, from 25 to 2 k Ω , with most of the reduction occurring over the first 20 pulses [Figure 4(a)]. After the pulsing, the resistance recovers slowly, reaching 7 k Ω in 1 h [Figure 4(b)].

Painless In Vivo Lateral Electroporation

The ERD was tested in vivo on a senior investigator, according to a protocol (protocol no. 2218) approved by the Institutional Review Board of the Massachusetts Institute of Technology (MIT) Committee on use of humans as experimental subjects. The subject's forearm was placed over the ERD, with the skin forming a tight seal around the openings in the gold electrode. The ERD (Figure 2) had an 11 \times 11 array of 65- μ m diameter microholes, with an annular gap between a microhole and the thin film gold electrode of 140 μ m and a microhole-to-microhole separation of 500 μ m. A series of 0.6-ms, 250-V exponential pulses was applied between the internal electrode and the gold film electrode. The skin impedance was reduced from 17 to 12 k Ω within the first ten pulses [Figure 4(c)]. The subject verbally reported the level of sensation experienced during pulsing. The subject felt no sensation during the ten pulses. However, as the annular gap between the gold surface and the edge of the opening in the PI sheet was increased, the sensation increased (Table 1). Although sensation evaluation was subjective, there was a clear transition from no sensation to various clear sensation levels, which is consistent with the ERD causing significant lateral electroporation (enhanced electric field confinement) and increasing amounts of transverse electroporation as the annular gap (half the differences in diameters) was increased. This result demonstrates that lateral skin electroporation that spans approximately 20 μ m thickness of the SC can be achieved by using field-confining electrodes. The data show that, for a certain range of microhole dimensions, the microconduits can be created painlessly. Such an approach may be amenable to a painless way of delivering drugs across human skin.

Transdermal Microscissioning

A micromechanical method of creating openings in skin using a mask to localize the intervention was also investigated. This method (microscissioning) uses moderate-velocity inert particles impinging stochastically on the skin to create 50–200- μ m diameter openings (microconduits). Microscissioning creates microconduits in human skin by incising the outer layers of skin using a gas-entrained stream of inert, sharp particles through a mask (Figure 5). The relatively hard, dry, roughened SC is removed by the sharp particles within the target area

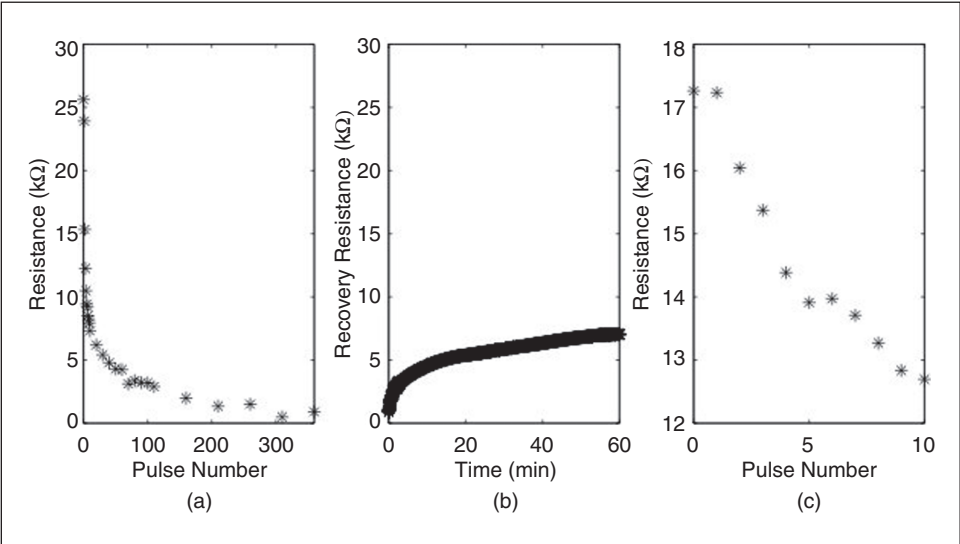


Fig. 4. Human skin electrical resistance after HV pulsing in vitro and in vivo, using a prototype ERD with an array (11 \times 11) of 121 microholes (65 μ m diameter; 50- μ m annular gap). (a) Decrease in resistance of in vitro full-thickness skin for 360 pulses. (b) Recovery of in vitro skin resistance after pulsing. (c) In vivo human forearm resistance decreases for ten pulses each of 250 V. The through-skin resistance was measured between the internal electrode of the ERD and a conventional ECG electrode at a hydrated skin site about 20 cm away (Figure 2). The subject felt no sensation. These results are consistent with localized electroporation of human skin in vitro.

[17]. By using a mask with microholes contacting the skin during the process, scissioning is confined to small areas of the skin. The mask also serves to limit the depth of intervention. The particles that bounce off the skin and skin fragments are removed by suction. If filled with saline, the electrical impedance between the microconduit and an unperturbed site on the skin can be used to gauge the depth of the microconduit.

Microscissioning Materials and Methods

The experimental setup used in the microscissioning study is shown in Figure 5. Experiments were performed using a modified Airbrasive model K, series II (S. S. White Technologies, Piscataway, NJ) instrument. The transdermal experiments were performed on senior investigators, according to a protocol approved by the MIT Committee on use of humans as experimental subjects. A hand-held unit containing multiple nozzles supporting moderate velocity flow of scissioning particles was coupled to a mask that contacted the subject's skin. A 75- μ m thick Kapton mask with one or four microholes with a specified diameter and center-to-center distance was used to constrain

Table 1. Painless-to-pain transition using an ERD with sterile saline.		
PI Microhole Diameter (μ m)	Gold Film Microhole Diameter (μ m)	Sensation
50	140	None
50	180	None
65	160 or 180	None
65	300	Very slight
65	500	Considerable
155	450 (7 \times 7 microhole array)	Sharp

the area of the skin exposed to the abrasive particles. The mask was mounted on a holder with a provision to position the gas nozzle directly above the mask. The device was connected by a hose to a reservoir of particles pressurized by a portable nitrogen gas cylinder. A vacuum attachment to the mask holder collected residual particles and skin fragments. Aluminum oxide (Al-602) (Atlantic Equipment Engineers, Bergensfield, NJ) was selected as the scissoring particle because of its inertness [22], size (20–70 μm), irregularity, and sharpness. The particles

in a nitrogen stream under a pressure of 550 kPa were directed toward a site on the inner left wrist, 10 cm from the center of the palm of the subject.

Microscissioned Microconduits

The use of a mask with an array of small openings of specified dimension and spacing enables the creation of well-defined microconduits in the skin. In addition, the use of multiple nozzles to direct the particle stream to localized sites on the skin

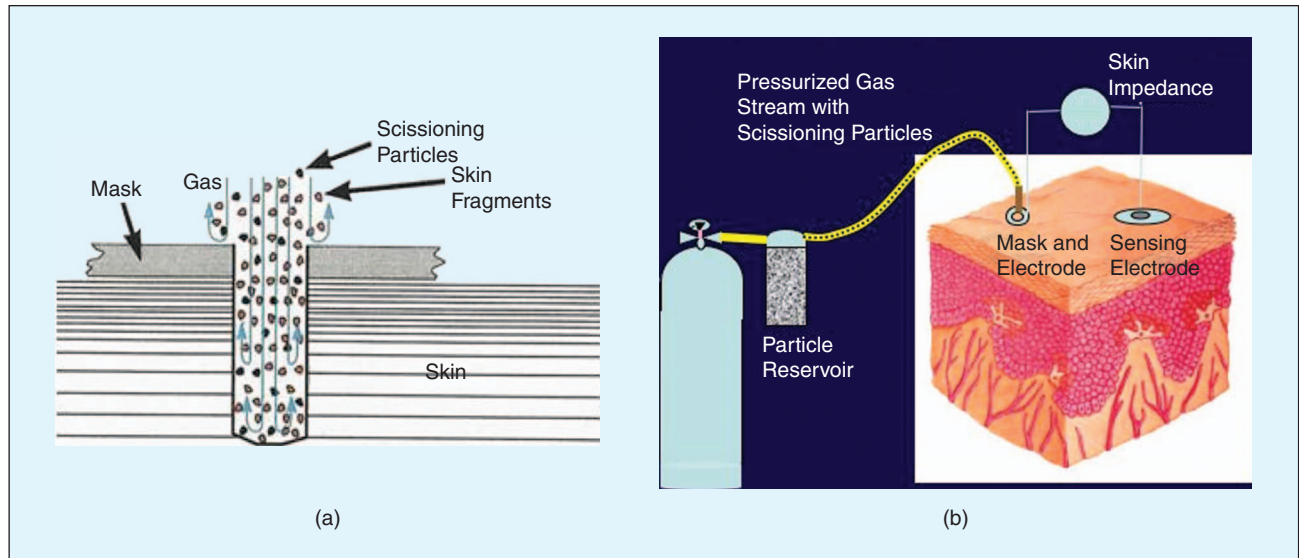


Fig. 5. (a) Microscissioning schematic. Microscissioning is achieved by a collimated flux of accelerated inert particles in a gas stream passing through the aperture in a mask held against the skin (17). The particles incise (cut) the tissue by removing the tissue fragments in the process, resulting in a microconduit that is fully open and is between 50 and 200 μm deep. (b) A 75- μm -thick Teflon mask with one or four holes, with a specified diameter and center-to-center distance, was used to constrain the area of the skin exposed to the abrasive particles. The mask was mounted on a holder, with the provision to position the gas nozzle directly above the mask. The mask with a single 200- μm diameter opening, a 450- μm diameter nozzle, and a nozzle to mask spacing of 1,500 μm was used. The particles in a nitrogen stream under a pressure of 550 kPa were directed toward a site on the inner left wrist, 10 cm away from the center of the palm of an adult subject. The depth of cut, saline-filled microconduits could be approximately controlled by monitoring the decrease of electrical impedance between an ECG electrode on the subject's unperturbed skin and the mask holder. A SR715 LCR meter operating at 1 V and 1 kHz was used to measure the skin impedance. The metal mask holder was electrically connected to the microconduit by saline contained in the conducting ring to which the mask was bonded. Since the mask was held tightly against the skin, the saline did not leak between the mask and skin, thus providing electrical continuity with the microconduit.

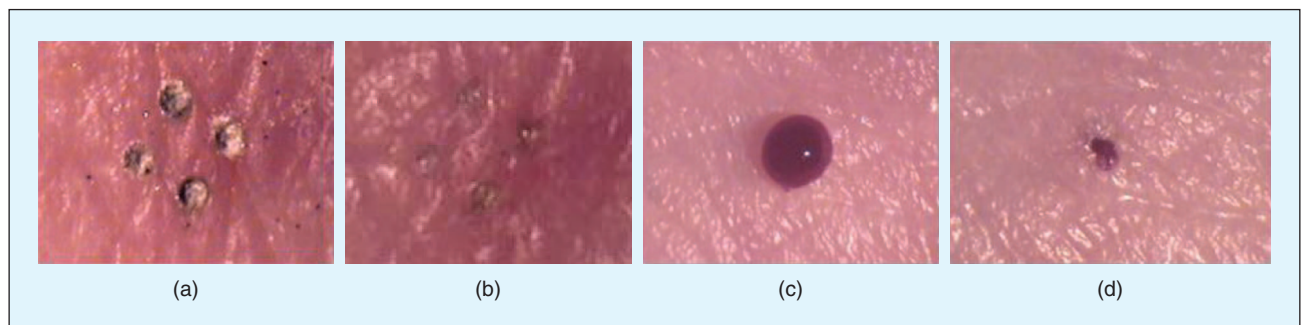


Fig. 6. Typical microconduits created by microscissioning (17). (a) A four-nozzle, four-hole mask was used to create a 2×2 array of microconduits 150 μm in diameter and 450 μm apart by microscissioning for 5 s. Some residual particles are seen within some of the microconduits. (b) On blowing the site gently with a stream of air and rinsing the site with saline, most of the particles are removed from the microconduit. (c) An example of a microconduit generated with a single hole in the mask. The scissoring time was increased to 18 s (for a single microconduit) to create a deeper microconduit that reached a blood vessel. A drop of blood is seen flowing out of the microconduit. This result shows that microconduits created by microscissioning may be useful for sampling blood and analytes. (d) The microconduit is shown after blotting out the blood drop.

ensures that different microconduits penetrate the skin to nearly identical depths. Typical microconduits created by a 2–5-s microscissioning procedure are shown in Figure 6. Immediately after the scissioning procedure, some particles are left inside the resulting microconduits [Figure 6(a)]. Blowing the site gently with a stream of air and rinsing the site with saline removed most of the particles from the microconduit [Figure 6(b)]. The impedance between the saline-filled microconduit site and an unperturbed site decreased from a prescissioning value of 2–3 M Ω to less than 100 k Ω . The depth of the microconduit was between 10 and 30 μ m. Extending the microscissioning procedure to a longer time created a deeper microconduit. For example, a 18-s procedure created a microconduit that was at least 100–160 μ m deep [Figure 6(c)]. The microconduit reached the depth of blood capillaries and reduced the skin impedance to 18–24 k Ω . Once the drop of blood emerging from the microconduit was

blotted out, the actual dimensions of the microconduit were evident [Figure 6(d)].

The process of microscissioning the outer layer of skin using accelerated sharp particles did not cause pain. For example, after a scissioning procedure that lasted for 7 s, the subject reported a pricking sensation. Even when a deeper microconduit was created with a visible blood drop at the site, the process was essentially pain-free, with a barely perceptible sensation attributed to the blood entering the tissue.

Recovery of Microconduits

Microscissioned sites were monitored for several days. Surrounding tissue and microconduits were imaged using an in vivo near-infrared reflectance-mode confocal microscope (Vivascope 1000) [23]. A mask with a 2 \times 2 array of 150- μ m microholes, 450 μ m apart, was used in creating a microconduit array. The resulting microconduits were approximately

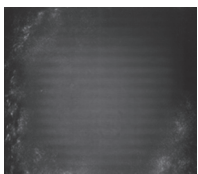
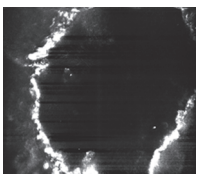
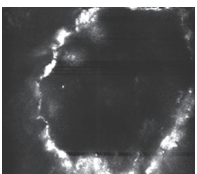
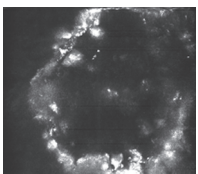
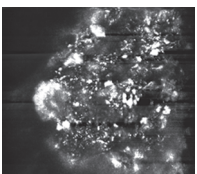
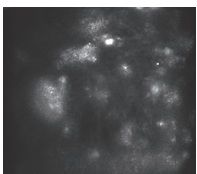
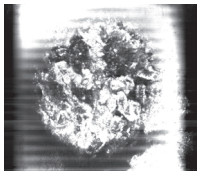
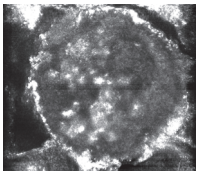
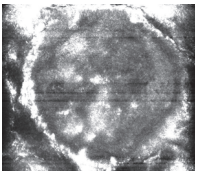
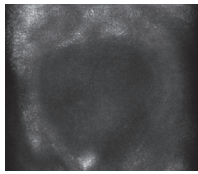
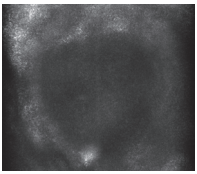
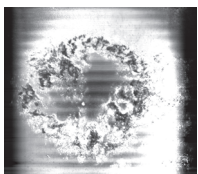
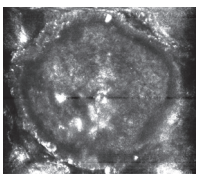
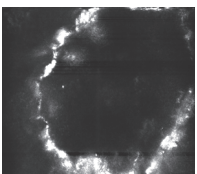
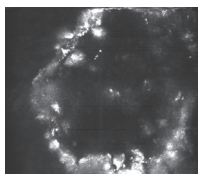
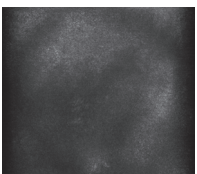
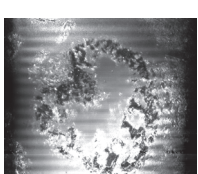
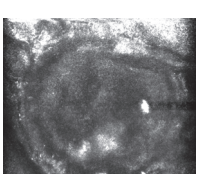
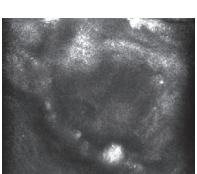
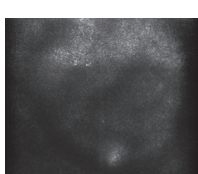
						
D0	Surface	20 μ m	48 μ m	66 μ m	88 μ m	132 μ m
						
D4	Surface	25 μ m	35 μ m	78 μ m	92 μ m	
						
D6	Surface	24 μ m	42 μ m	59 μ m	86 μ m	
						
D8	Surface	25 μ m	43 μ m	73 μ m		

Fig. 7. Recovery of microconduits. Microconduits were imaged using a Vivascope 1000 (Lucid, Rochester, NY) in vivo near-infrared reflectance-mode confocal microscope, with an 830 nm illumination wavelength, 30 mW power, and a 30 \times , 0.9 numerical aperture (NA) water immersion objective lens. Images were taken at different focal planes showing the microconduit at different depths from the surface of the skin. Images were acquired on several days following microscissioning. Each row of images shows the depth profile of the microconduit on different days (indicated on the left). It is seen that immediately after microscissioning, the microconduit is at least 130 μ m deep, with residual particles seen at around 90 μ m deep. As the days progress, the residual particles are carried outward and the depth of the microconduit begins to decrease. On day 8, very few particles are seen in the microconduit that is now only 70 μ m deep.

160 μm in diameter. One of these four microconduits is shown in Figure 7. Images were taken at different focal planes, showing the microconduit at different depths from the surface of the skin. It is seen that, immediately after microscissioning, the microconduit was at least 130 μm deep, with the residual particles being seen at about 90 μm depth. The particles left in the microconduit were tracked several days after. As time progressed, the residual particles were carried outward and the depth of the microconduit began to decrease. By day 8, very few particles were seen in the microconduit, which was now only 70 μm deep.

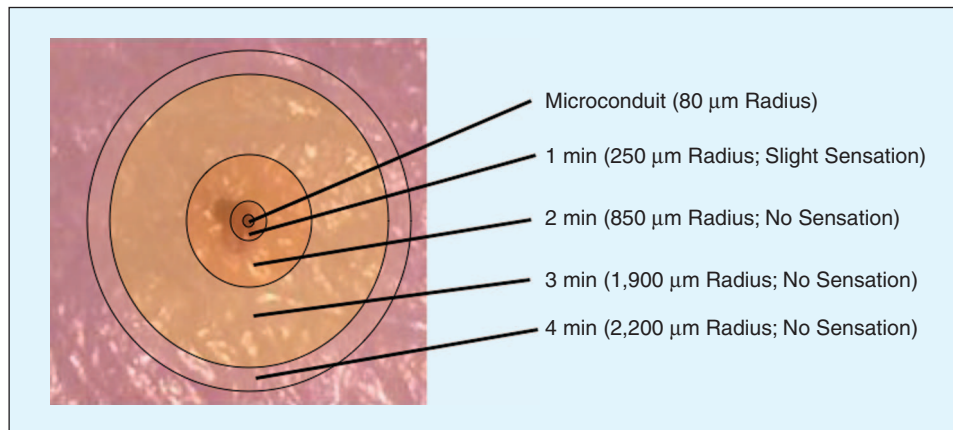


Fig. 8. Transdermal lidocaine delivery. A single 160- μm diameter, 100–150- μm deep microconduit was created by microscissioning. A cotton pad saturated with 50% lidocaine applied over the microconduit site showed a clear decrease in sensation in less than 2 min. In 4 min, the anesthetized radius increased to 2.8–3 mm. This contrasts with the 60–90-min duration it takes for passive delivery of lidocaine to take effect.

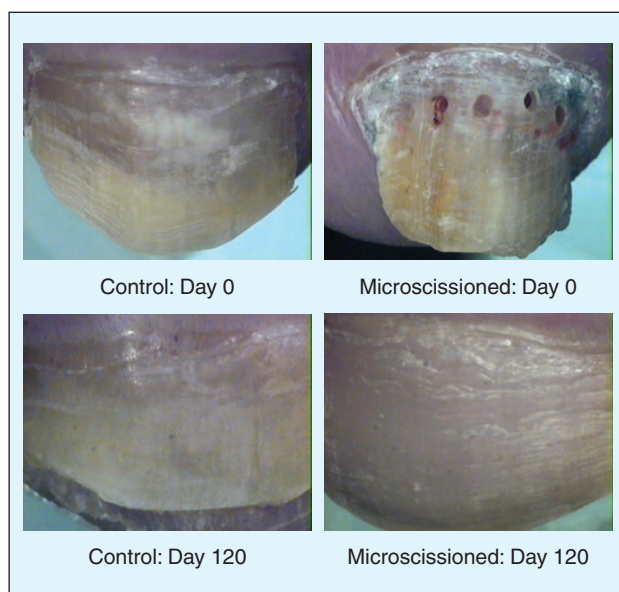


Fig. 9. Ungual drug delivery: Four microconduits were microscissioned in the toenail of a subject with onychomycosis. The subject did not feel any sensation during the creation of microconduits. Lamisil (1%) cream was applied over the microconduits once every two days for four months. The thickness of the treated nail returned to a normal value at the end of four months. Also, the treated nail showed no discoloration from fungal infection four months from the start of the treatment.

Transdermal Delivery of Lidocaine

Transdermal drug delivery through microscissioned microconduits was investigated by delivering lidocaine, a local anesthetic [17]. A mask with a single 160- μm diameter microhole was used. Lidocaine (50% solution: 5 g lidocaine hydrochloride in 5 mL normal saline) was topically applied over the microconduit site and a control site in saturated filter paper pads with Finn chambers taped over each site for 5 min. A pin stick test for sensation was used to determine the minimum time for full anesthetic effect. Here, the subject's skin was probed with a sharp pin at different distances from the microconduit (or center of control site) at different times after microscissioning. The test was done on a single 160- μm diameter microconduit, 100–150- μm deep on the left inner wrist.

Microscissioning created a 160- μm diameter, 100–150- μm deep microconduit. A cotton pad saturated with 50% lidocaine applied over the microconduit site showed a clear decrease in sensation in less than 2 min (Figure 8). In 4 min, the anesthetized region's radius increased to 2.8–3 mm with complete numbness. This contrasts with the 60–90-min duration it takes for passive delivery of lidocaine to take effect [25]. The anesthetic effect lasted for more than 1 h in this region.

Ungual Drug Delivery

Topical delivery of medications to treat nail fungal infection and nail psoriasis is largely ineffective because of the poor permeability of fingernails and toenails to such drugs [26]–[28]. Most of the approaches developed for transdermal drug delivery are not suited for enhancing drug delivery through nail. Different types of pulsed laser systems have been used to ablate nail [29]. Ungual microconduits (openings in nail) created by microscissioning offer pathways for effective delivery of medications to the underlying nail bed (transungual drug delivery). Four microconduits were microscissioned in the toenail of a senior investigator (Figure 9). The subject did not feel any sensation during the creation of microconduits. An antifungal drug, 1% Lamisil cream (terbinafine hydrochloride), was introduced into the microconduits once every day for more than four months. The thickness of treated nail returned to a normal value at the end of four months. Also, the treated nail showed no discoloration associated with fungal infection four months into treatment.

Conclusions

Both field-confined skin electroporation and microscissioning offer minimally invasive methods for delivering drugs across skin and nail with minimal sensation [16]. Both methods create high permeability pathways in a pain-free manner. These openings are similar in dimension to commonly experienced scratches and nicks on the skin. These localized openings provide pathways for sustained delivery of drugs either passively using a patch or actively using pressure or iontophoresis.

Acknowledgments

The authors are grateful to R. R. Anderson, S. Gonzalez, U. Pliquet, M. Rajadhyaksha, and R. Tachihara for their assistance and useful discussions. This research was supported by grants from MIT Lincoln Laboratory and National Institutes of Health (NIH; RO1-AR4921 and RO1-GM6387), with additional support from Massachusetts General Hospital and Center for Integration of Medicine and Innovative Technology (CIMIT).



T. R. Gowrishankar received his B.E. degree from Bangalore University, India, in 1986, an M.S. degree from George Mason University, Fairfax, Virginia, in 1989, and a Ph.D. degree in medical physics from the University of Chicago, Illinois, in 1996. He is currently a research scientist at the Harvard-MIT Division of Health Sciences and Technology at the MIT, Cambridge. He is also the vice president of R&D at Carlisle Scientific Inc. and Path Scientific Inc. in Carlisle, Massachusetts. His research interests include experimental and simulation studies of bioelectric phenomena, drug delivery, and medical devices.



Terry O. Herndon received his B.S. degree in electrical engineering from the Antioch College in 1957. He was a research staff in MIT Lincoln Laboratory for more than 40 years. He holds more than a dozen patents in integrated circuit fabrication and medical technologies. He developed electronic chips to act as light sensors and power source for artificial retina. He has published many research papers on integrated circuit fabrication techniques and drug-delivery methods. He has served on the editorial board of the Electrochemical Society. He is the founding president of two drug delivery companies, Carlisle Scientific and Path Scientific in Carlisle, Massachusetts. His research interests include drug delivery, medical devices, and microelectronics.

James C. Weaver Photograph and biography not available.

Address for Correspondence: James C. Weaver, MIT, E25-213A, 77 Massachusetts Avenue, Cambridge, MA 02139, USA. E-mail: jcw@mit.edu.

References

- [1] M. R. Prausnitz, S. Mitragotri, and R. Langer, "Current status and future potential of transdermal drug delivery," *Nat. Rev. Drug Discov.*, vol. 3, no. 2, pp. 115–121, 2004.
- [2] S. E. Cross and M. S. Roberts, "Physical enhancement of transdermal drug application: Is delivery technology keeping up with pharmaceutical development?" *Curr. Drug Deliv.*, vol. 1, pp. 81–92, Jan. 2004.
- [3] P. Karande, A. Jain, K. Ergun, V. Kispersky, and S. Mitragotri, "Design principles of chemical penetration enhancers for transdermal drug delivery," *Proc. Natl. Acad. Sci. USA*, vol. 102, pp. 4688–4693, Mar. 2005.
- [4] P. Karande, A. Jain, and S. Mitragotri, "Discovery of transdermal penetration enhancers by high-throughput screening," *Nat. Biotech.*, vol. 22, no. 2, pp. 192–197, 2004.
- [5] Y. N. Kalia, A. Naik, J. Garrison, and R. H. Guy, "Iontophoretic drug delivery," *Adv. Drug Deliv. Rev.*, vol. 56, pp. 619–658, Mar. 2004.
- [6] I. Lavon and J. Kost, "Ultrasound and transdermal drug delivery," *Drug Discov. Today*, vol. 9, pp. 670–676, Aug. 2004.
- [7] S. Mitragotri and J. Kost, "Low-frequency sonophoresis: A review," *Adv. Drug Deliv. Rev.*, vol. 56, pp. 589–601, Mar. 2004.
- [8] J. Bramson, K. Dayball, C. Eveleigh, Y. H. Wan, D. Page, and A. Smith, "Enabling topical immunization via microporation: A novel method for pain-free and needle-free delivery of adenovirus-based vaccines," *Gene Ther.*, vol. 10, pp. 251–260, Feb. 2003.
- [9] J. Y. Fang, W. R. Lee, S. C. Shen, H. Y. Wang, C. L. Fang, and C. H. Hu, "Transdermal delivery of macromolecules by erbium:YAG laser," *J. Control. Release*, vol. 100, pp. 75–85, Nov. 2004.
- [10] D. V. McAllister, P. M. Wang, S. P. Davis, J. H. Park, P. J. Canatella, M. G. Allen, and M. R. Prausnitz, "Microfabricated needles for transdermal delivery of macromolecules and nanoparticles: Fabrication methods and transport studies," *Proc. Natl. Acad. Sci. USA*, vol. 100, pp. 13755–13760, Nov. 2003.
- [11] S. P. Davis, W. Martanto, M. G. Allen, and M. R. Prausnitz, "Hollow metal microneedles for insulin delivery to diabetic rats," *IEEE Trans. Biomed. Eng.*, vol. 52, pp. 909–915, May 2005.
- [12] S. Wang, S. Joshi, and S. Lu, "Delivery of DNA to skin by particle bombardment," *Methods Mol. Biol.*, vol. 245, pp. 185–196, 2004.
- [13] T. R. Gowrishankar, T. O. Herndon, T. E. Vaughan, and J. C. Weaver, "Spatially constrained localized transport regions due to skin electroporation," *J. Control. Release*, vol. 60, no. 1, pp. 101–110, 1999.
- [14] L. Ilic, T. R. Gowrishankar, T. E. Vaughan, T. O. Herndon, and J. C. Weaver, "Spatially constrained skin electroporation with sodium thiosulfate and urea creates transdermal microconduits," *J. Control. Release*, vol. 61, no. 1–2, pp. 185–202, 1999.
- [15] L. Ilic, T. R. Gowrishankar, T. E. Vaughan, T. O. Herndon, and J. C. Weaver, "Microfabrication of individual 200 μm diameter transdermal microconduits using high-voltage pulsing in salicylic acid and benzoic acid," *J. Inv. Dermatol.*, vol. 116, pp. 40–49, Jan. 2001.
- [16] U. F. Pliquet and J. C. Weaver, "Feasibility of an electrode-reservoir device for transdermal drug delivery by non-invasive skin electroporation," *IEEE Trans. Biomed. Eng.*, vol. 54, no. 3, pp. 536–538, 2007.
- [17] T. O. Hendon, S. Gonzalez, T. R. Gowrishankar, R. R. Anderson, and J. C. Weaver, (2004). "Transdermal microconduits by microscission for drug delivery and sample acquisition," *BMC Med.* [Online]. Available: <http://www.biomedcentral.com/1741-7015/2/12>
- [18] M. R. Prausnitz, V. G. Bose, R. Langer, and J. C. Weaver, "Electroporation of mammalian skin: A mechanism to enhance transdermal drug delivery," *Proc. Natl. Acad. Sci. USA*, vol. 90, no. 22, pp. 10504–10508, 1993.
- [19] J. C. Weaver and Y. A. Chizmadzhev, "Theory of electroporation: A review," *Bioelectrochem. Bioenerg.*, vol. 41, no. 2, pp. 135–160, 1996.
- [20] J. C. Weaver, T. E. Vaughan, and Y. A. Chizmadzhev, "Theory of electrical creation of aqueous pathways across skin transport barriers," *Adv. Drug Deliv. Rev.*, vol. 35, no. 1, pp. 21–39, 1999.
- [21] T. E. Zewert, U. Pliquet, R. Vanbever, R. Langer, and J. C. Weaver, "Creation of transdermal pathways for macromolecule transport by skin electroporation and a low toxicity, pathway-enlarging molecule," *Bioelectrochem. Bioenerg.*, vol. 49, no. 1, pp. 11–20, 1999.
- [22] P. S. Christel, "Biocompatibility of surgical-grade dense polycrystalline alumina," *Clin. Orthop.*, vol. 282, pp. 10–18, 1992.
- [23] M. Rajadhyaksha, S. Gonzalez, J. M. Zavislan, R. R. Anderson, and R. H. Webb, "In vivo confocal scanning laser microscopy of human skin. II. Advances in instrumentation and comparison with histology," *J. Invest. Dermatol.*, vol. 113, no. 6, pp. 293–303, 1999.
- [24] E. Hernández, S. González, and E. González, "Evaluation of topical anesthetics by laser-induced sensation: Comparison of EMLA 5% cream and 40% lidocaine in an acid mantle ointment," *Laser Surg. Med.*, vol. 23, no. 3, pp. 167–171, 1998.
- [25] L. Arendt-Nielsen and P. Bjerring, "The effect of topically applied anaesthetics (EMLA cream) on thresholds to thermode and argon laser stimulation," *Acta Anaesth. Scand.*, vol. 33, no. 6, pp. 469–473, 1989.
- [26] X. Hui, Z. Shainhouse, H. Tanojo, A. Anigbogu, G. E. Markus, H. I. Maibach, and R. C. Wester, "Enhanced human nail drug delivery: Nail inner drug content assayed by new unique method," *J. Pharm. Sci.*, vol. 91, no. 1, pp. 189–195, 2002.
- [27] Y. Kobayashi, T. Komatsu, M. Sumi, S. Numajiri, M. Miyamoto, D. Kobayashi, K. Sugibayashi, and Y. Morimoto, "In vitro permeation of several drugs through the human nail plate: Relationship between physicochemical properties and nail permeability of drugs," *Eur. J. Pharm. Sci.*, vol. 21, no. 4, pp. 471–477, 2004.
- [28] S. Murdan, "Drug delivery to the nail following topical application," *Int. J. Pharm.*, vol. 236, no. 1–2, pp. 1–26, 2002.
- [29] J. S. Neev, J. S. Nelson, M. Critelli, J. L. McCullough, E. Cheung, W. A. Carrasco, A. M. Rubenchik, L. B. De Silva, M. D. Perry, and B. C. Stuart, "Ablation of human nail by pulsed lasers," *Laser Surg. Med.*, vol. 21, no. 2, pp. 186–192, 1997.
- [30] T. R. Gowrishankar and J. C. Weaver, "An approach to electrical modeling of single and multiple cells," *Proc. Natl. Acad. Sci. USA*, vol. 100, no. 6, pp. 3203–3208, Mar. 2003.
- [31] U. F. Pliquet, G. T. Martin, and J. C. Weaver, "Kinetics of the temperature rise within human stratum corneum during electroporation and pulsed high-voltage iontophoresis," *Bioelectrochem. Bioenerg.*, vol. 57, no. 1, pp. 65–72, 2002.